Generation of entangled photon pairs using small-coherence-time continuous wave pump lasers

Simone Cialdi,[1,*] Fabrizio Castelli,[1,2] Ilario Boscolo,[1,2] and Matteo G. A. Paris[2,3,4]

[1]Instituto Nazionale di Fisica Nucleare (INFN), Sezione di Milano, via Celoria 16, Milano I-20133, Italy

[2]Dipartimento di Fisica dell'Università di Milano, via Celoria 16, Milano I-20113, Italy

[3]Institute for Scientific Interchange Foundation, I-10133 Torino, Italy

[4]Consorzio Nazionale Interuniversitario per le Scienze Fisiche della Materia (CNISM), Sezione di Milano I-20133, Italy

*Corresponding author: simone.cialdi@mi.infn.it

Received 12 November 2007; revised 17 January 2008; accepted 18 January 2008;
posted 18 January 2008 (Doc. ID 89588); published 8 April 2008

We address the generation of entangled photon pairs by parametric downconversion from solid state cw lasers with small coherence time. We consider a compact and low-cost setup based on a two-crystal scheme with type-I phase matching. We reconstruct the full density matrix by quantum tomography and analyze in detail the entanglement properties of the generated state as a function of the crystal's length and the coherence time of the pump. We verify the possibility to improve the visibility using a purification protocol based on a compensation crystal. © 2008 Optical Society of America

OCIS codes: 270.1670, 270.5290.

1. Introduction

The generation of entanglement is the key ingredient of quantum information processing. In optical implementation with discrete variables the standard source of entangled photon pairs is parametric downconversion in nonlinear crystals pumped by single-mode lasers [1]. Recent advances in laser diode technology allow the realization of simpler and cheaper apparatus for the entanglement generation [2], though the quality of the resulting photon pairs is degraded by the small coherence time of the pump laser.

In this paper we present a detailed characterization of the entangled state produced by downconversion with the laser diode pump. We reconstruct the full density matrix by quantum tomography and analyze in detail the properties of the generated state, including purity and visibility, as a function of the crystal's length and the coherence time of the pump. We also verify the possibility to improve the visibility using a purification protocol based on a compensation crystal [3]. The topics are relevant for application for at least two reasons. On the one hand quantifying the degree of entanglement is of interest in view of a large scale application. On the other hand a detailed characterization of the generated state allows one to suitably tailor entanglement distillation protocols.

2. Results and Discussion

Besides standard visibility tests, we characterize the generated states by full quantum tomography of their density matrices [4]. Upon measuring a set of independent projectors $P_\mu = |\psi_\mu\rangle\langle\psi_\mu| (\mu = 1, ..., 16)$ corresponding to different combinations of polarizers and phase shifters, the density matrix may be reconstructed as $\varrho = \sum_\mu p_\mu \Gamma_\mu$, where $p_\mu = \mathrm{Tr}[\varrho P_\mu]$ are the probabilities of getting a count when measuring P_μ and Γ_μ the corresponding dual basis, i.e., the set of operators satisfying $\mathrm{Tr}[P_\mu \Gamma_\nu] = \delta_{\mu\nu}$ [5]. Of course in the experimental reconstruction the probabilities p_μ are substituted by their experimental samples, i.e., the frequencies of counts obtained when measuring P_μ. To minimize the effects of fluctuations

0003-6935/08/111832-05$15.00/0

and avoid nonphysical results we use maximum-likelihood reconstruction of two-qubit states [6,7]. Results of the reconstruction are reported for crystals with three different thicknesses and in the case of compensation of the delay time between generated photons.

Figure 1 is a schematic of the experimental system. The "state generator" consists of two identical β-barium borate (BBO) crystals, each cut for type-I downconversion, one half-wave plate (HWP) and one quarter-wave plate (QWP) as in [8]. The crystals are stacked back-to-back, with their axes oriented at 90° with respect to each other [1,2]. The balancing and the phase of the entangled states are selected by changing the HWP and QWP orientation. The crystals are pumped using a 40 mW, 405 nm laser diode (Newport LQC405-40P) with a coherence time τ_c of 544 fs (we obtained this information by measuring the first-order correlation function). The generated photons are analyzed using adjustable QWP, HWP, and a polarizer [7]. Finally light is focused into multimode fibers that are used to direct the photons to the detectors. The detectors are homemade single photon counting modules (SPCM) based on an avalanche photodiode operated in the Geiger mode with active quenching. For the coincidence counting we use a time-to-amplitude converter/single-channel analyzer (TAC/SCA).

As sketched in Fig. 2, the first crystal converts horizontally polarized pump photons into vertically polarized (V) signal and idler, while the second crystal converts vertically polarized pump photons into horizontally polarized (H) signal and idler. This configuration introduces a delay time $\Delta\tau$ between the V and the H part of the entangled state, depending on the crystal length. The nonlinear crystals are properly cut to generate photons into a cone of a half-opening angle of 3° with respect to the pump.

We performed three series of measurements using crystals of different thicknesses: 0.5, 1, and 3 mm. The state reconstruction for the three cases is shown in Fig. 3. As explained below, for the 0.5 mm crystals the delay time $\Delta\tau$ is lower than the coherence time τ_c of the pump laser, and the generated entangled state is characterized by high purity. In the case of 1 mm crystals, the delay time is of the same order of τ_c, and

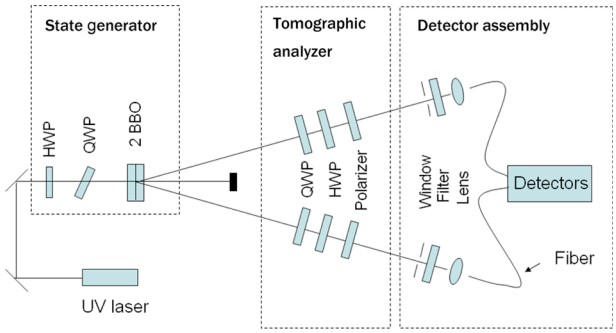

Fig. 1. (Color online) Experimental apparatus for generating and analyzing entangled states.

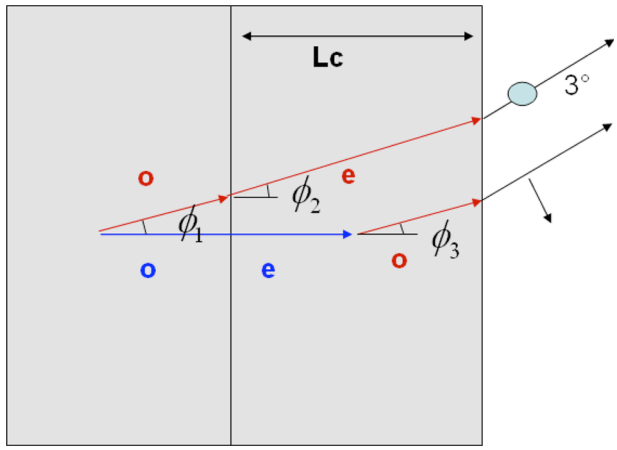

Fig. 2. (Color online) Entangled photon generation and propagation inside the crystals. For clarity, only signal photon trajectories are drawn. o and e indicate ordinary and extraordinary rays, respectively; L_c is the length of both crystals.

the purity is degraded with respect to the previous case. For 3 mm crystals one has $\Delta\tau > \tau_c$, and the nondiagonal elements of the density matrix, as well as the entanglement, are washed out.

3. Theoretical Model and Discussion

A theoretical description of this behavior can be given using the interaction picture. The state produced by spontaneous parametric downconversion (SPDC) can be written (to first order in perturbation [9,10]) as $|\Psi\rangle = \int \mathrm{d}\omega_p \mathrm{d}\omega f(\omega_p,\omega) A(\omega_p) |P,\omega\rangle_s |P,\omega_p-\omega\rangle_i$, where ω_p and ω are the offset with respect to the pump central frequency Ω_p and the SPDC central frequency $\Omega = \Omega_p/2$. $A(\omega_p)$ is the complex amplitude of the pump laser, $|P,\omega\rangle_{s,i}$ is a normalized state vector (with P polarization) for signal (s) or idler (i) photons, and f is the function that contains the phase mismatch between radiation modes: $f(\omega_p,\omega) = \sin(\frac{1}{2}\Delta k L_c)/(\frac{1}{2}\Delta k L_c)$, $(\Delta k = k_p - k_s - k_i)$.

In our configuration the wave function rewrites as

$$|\Psi\rangle = \int \mathrm{d}\omega_p \mathrm{d}\omega f(\omega) A(\omega_p) \times \frac{1}{\sqrt{2}} [e^{-i\phi_H - i\omega_p\tau_H} |H,\omega\rangle_s |H,\omega_p-\omega\rangle_i + e^{-i\phi_V - i\omega_p\tau_V} |V,\omega\rangle_s |V,\omega_p-\omega\rangle_i], \quad (1)$$

where $e^{-i\phi_H - i\omega_p\tau_H}$ and $e^{-i\phi_V - i\omega_p\tau_V}$ are signal and idler propagators inside crystals under the approximation in which photons are assumed generated in the crystal's middle [11,12]. We discarded the dependence of the mismatch function f on ω_p; in our case the goodness of this approximation may be easily tested numerically. Referring to Fig. 2 the propagation times are given by

$$\tau_V = \frac{1}{2}\frac{L_c}{\cos(\phi_1) V^{(o)}_{\mathrm{SPDC}}} + \frac{L_c}{\cos(\phi_2) V^{(e)}_{\mathrm{SPDC}}}, \quad (2)$$

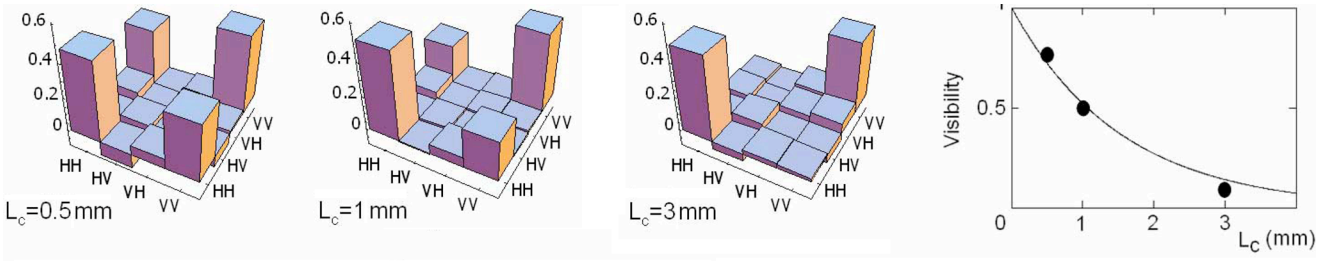

Fig. 3. (Color online) Tomographic reconstruction of the generated state for three different crystals. In the fourth plot we show the calculated visibility (curve) as well as the values (full circles) obtained from the reconstructed density matrix for the three crystal pairs: 0.77 visibility for 0.5 mm crystals, 0.50 for 1 mm, and 0.09 for 3 mm.

$$\tau_H = \frac{1}{2}\frac{L_c}{V^{(o)}_{\text{pump}}} + \frac{1}{2}\frac{L_c}{V^{(e)}_{\text{pump}}} + \frac{1}{2}\frac{L_c}{\cos(\phi_3)V^{(o)}_{\text{SPDC}}}, \tag{3}$$

where $V^{(o,e)}_{\text{pump,SPDC}}$ are group velocities and the angles ($\phi_1 = 1.807$, $\phi_2 = 1.84$, and $\phi_3 = 1.806$) are determined by the request of the 3° exit angle for signal and idler. Data on group velocities are taken from [13]; the angles ϕ_1 and ϕ_2 can be found from the laws of wave propagation in birefringent crystals [14] while ϕ_3 is simply given by Snell's law. We disregard the angular dependence due to detector transverse dimension because our fiber collimators cover a very small area (~1.5 mm) of the SPDC. Besides, having a laser spot with a 2 mm diameter, we also consider exact transverse momentum conservation [15].

The calculation of the elements of the density matrix operator in the polarization bases (HH, HV, VH, VV) straightforwardly proceeds using the orthogonality relations $\langle P,\omega|Q,\omega'\rangle = \delta_{P,Q}\delta(\omega-\omega')$, because with a cw pump laser one has

$$\int d\omega_p A(\omega_p) e^{-i\omega_p t} = A_0 e^{i\delta(t)}, \tag{4}$$

where A_0 is a constant amplitude and $\delta(t)$ is the laser phase fluctuating with the coherence time τ_c. Using the state vectors defined herein, the desired density matrix is given by multiple integration over state frequencies

$$\rho = \int d\omega_p' d\omega_i' \langle \omega_p' - \omega'|_s \langle \omega'|\Psi\rangle \times \langle \Psi|\omega'\rangle_s |\omega_p' - \omega'\rangle_i. \tag{5}$$

Only four elements are different from zero; the first is

$$\rho_{HH,HH} = \frac{1}{2}\int d\omega |f(\omega)|^2 \int d\omega_p |A(\omega_p)|^2 = \frac{1}{2}\epsilon A_0^2 \frac{\Delta T}{2\pi}, \tag{6}$$

where we put $\epsilon = \int d\omega |f(\omega)|^2$ with a constant ϵ and $\int d\omega_p |A(\omega_p)|^2 = A_0^2 \frac{\Delta T}{2\pi}$ where ΔT is a large time interval. With similar calculations we obtain $\rho_{VV,VV} = \rho_{HH,HH}$. The other two elements are off diagonal and read

$$\begin{aligned}\rho_{HH,VV} &= \frac{1}{2}\int d\omega |f(\omega)|^2 \\ &\quad \times \int d\omega_p |A(\omega_p)|^2 e^{-i(\phi_H-\phi_V)} e^{-i\omega_p(\tau_H-\tau_V)} \\ &= \frac{1}{2}\epsilon e^{-1\phi}\int d\omega_p |A(\omega_p)|^2 e^{-i\omega_p(\tau_H-\tau_V)} \\ &= \rho^*_{VV,HH},\end{aligned} \tag{7}$$

where $\phi = \phi_H - \phi_V$.

With the Wiener–Khinchin theorem the frequency integral can be recast as a two time correlation function over the interval ΔT, very large with respect to the coherence time of the pump and smaller than the detector characteristic time:

$$\begin{aligned}&\int d\omega_p |A(\omega_p)|^2 e^{-i\omega_p(\tau_H-\tau_V)} = A_0^2 \frac{\Delta T}{2\pi} \\ &\times \left(\frac{1}{\Delta T}\int_{\Delta T} dt e^{-i\delta(t)+\delta[t-(\tau_H-\tau_V)]}\right) = A_0^2 \frac{\Delta T}{2\pi} e^{-\frac{\Delta\tau}{\tau_c}},\end{aligned} \tag{8}$$

where $\Delta\tau = |\tau_H - \tau_V|$ and the result is taken from [16]. If $\Delta\tau \gg \tau_c$ we have an incoherent superposition of random phases, and the average of the complex exponentials tends to zero, otherwise we have a coherent sum, and the integral tends to one.

Finally, setting the state generator QWP to have $\phi = 0$ (see [1]) we get a density matrix with real elements, which explicitly read

$$\begin{array}{c} \\ HH \\ HV \\ VH \\ VV \end{array} \begin{array}{c} \begin{array}{cccc} HH & HV & VH & VV \end{array} \\ \begin{bmatrix} \frac{1}{2} & 0 & 0 & \frac{1}{2}e^{-\Delta\tau/\tau_c} \\ 0 & 0 & 0 & 0 \\ 0 & 0 & 0 & 0 \\ \frac{1}{2}e^{-\Delta\tau/\tau_c} & 0 & 0 & \frac{1}{2} \end{bmatrix} \end{array}. \tag{9}$$

It is clear that the ratio $\Delta\tau/\tau_c$ governs the visibility of the entangled state. In fact, from Eqs. (2) and (3) the delay time results $\Delta\tau = 355 L_c$ fs and becomes larger than $\tau_c = 544$ fs only for a crystal length greater than 2 mm, destroying the nondiagonal elements and introducing decoherence as shown by the experimental results. The theoretical visibility of the entangled state is calculated from Eq. (9) as $\exp(-\Delta\tau/\tau_c)$ as

shown in Fig. 3. Also indicated in Fig. 3 are the reconstructed visibilities for the three crystal pairs.

In our model the lack of purity of the entangled state is fully ascribed to the fluctuating phase difference between the H and the V parts of the SPDC, linked to delay $\Delta\tau$. Having a very small area of the fiber collimator, we have neglected any decoherence of spatial origin that introduces a phase variation depending on the detector viewing angle. To verify this statement, we performed a series of measurements with the 3 mm crystal, putting windows of 0.5 mm linear aperture in front of the collimators. If the decoherence had a spatial contribution, we would have expected an increase in the purity. In fact, the results of the state reconstruction were the same as the original configuration thus supporting our hypothesis.

This fact also suggests how to improve the purity of the entangled state by a phase retardation on the H polarized part of the pump with respect to the V polarized part [3]. This can be accomplished by inserting, along the pump ray and before the state generator, a properly oriented birefringent crystal with a suitable length. In this way we introduce two different delay times τ_H^c and τ_V^c on the pump, with $\tau_H^c - \tau_V^c = (\frac{1}{V_H^c} - \frac{1}{V_V^c})L_{\mathrm{comp}}$, where L_{comp} is the compensation crystal length, and V_H^c and V_V^c are the pump group velocities. These delays must be summed to the original delay times τ_H and τ_V to obtain a new $\Delta\tau = |\tau_H - \tau_V + \tau_H^c - \tau_V^c|$, which must be set equal to zero to obtain maximum visibility. This condition of perfect compensation requires selecting proper crystal length and orientation.

With the BBO crystals used in our laboratory it was possible to achieve partial compensation and only in one selected configuration. We performed a series of measurements using the 1 mm double crystal as the state generator and a 3 mm single crystal as the pump phase retarder. The length of this crystal is very near to the ideal one, but we cannot select the better orientation for the principal axis because it is much too similar to the phase matching angle for the SPDC generation.

The visibility is expected to vary from a maximum to a minimum for a 90° change in compensation crystal orientation with respect to the longitudinal axis as confirmed by the tomographic reconstruction shown in Fig. 4. The maximum visibility of 0.66 is larger than the corresponding visibility without the auxiliary crystal (see Fig. 3) thus demonstrating a partial time delay compensation.

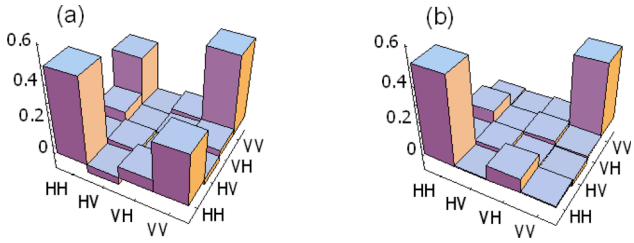

Fig. 4. (Color online) Tomographic reconstruction with a delay compensation crystal (see text). (a) Crystal angle set for maximum compensation, visibility 0.66. (b) Crystal angle at 90° with respect to (a), visibility 0.17.

4. Conclusion

In summary, we have analyzed the process of decoherence of an entangled state due to the temporal delay inherent in the process of creating photons via parametric downconversion in a two-crystal configuration. We related it to the coherence properties of the pump laser and obtained good agreement between experimental results and a suitable theoretical model using different crystals. A purification scheme based on a compensation crystal introducing a time delay opposite the generation was employed to verify the proposed model. We finally note that, in our experimental configuration, by using crystals with a suitable length, it is possible to directly generate a mixed state (with a density matrix equal to $\frac{1}{2}(|HH\rangle\langle HH| + |VV\rangle\langle VV|)$ without introducing electro-optic elements before the state generator [8].

This work has been supported by Ministry of Education, University, and Research (MIUR) project PRIN2005024254-002. M. G. A. Paris acknowledges useful discussions with Maria Bondani. We are also indebted to Stefano La Torre for his help with detector realization.

References

1. P. G. Kwiat, E. Waks, A. G. White, I. Appelbaum, and P. G. Eberhard, "Ultrabright source of polarization-entangled photons," Phys. Rev. A **60**, R773–R776 (1999).
2. D. Dehlinger and M. W. Mitchell, "Entangled photons, nonlocality, and Bell inequalities in the undergraduate laboratory," Am. J. Phys. **70**, 903–910 (2002).
3. Y. Nambu, K. Usami, Y. Tsuda, K. Matsumoto, and K. Nakamura, "Generation of polarization-entangled photon pairs in a cascade of two type-I crystals pumped by femtosecond laser pulses," Phys. Rev. A **66**, 033816 (2002)
4. M. G. A. Paris and J. Rehacek, eds., "Quantum state estimation," Lect. Notes Phys. **649**, 1–4 (2004).
5. G. M. D'Ariano, L. Maccone, and M. G. A. Paris, "Quorum of observables for universal quantum estimation," J. Phys. A **34**, 93–104 (2001).
6. K. Banaszek, G. M. D'Ariano, M. G. A. Paris, and M. F. Sacchi, "Maximum-likelihood estimation of the density matrix," Phys. Rev. A **61**, 010304 (2000).
7. D. F. V. James, P. G. Kwiat, W. J. Munro, and A. G. White, "Measurement of qubits," Phys. Rev. A **64**, 052312 (2001).
8. A. Gogo, W. D. Snyder, and M. Beck, "Comparing quantum and classical correlations in a quantum eraser," Phys. Rev. A **71**, 052103 (2005).
9. M. H. Rubin, D. N. Klyshko, Y. H. Shih, and A. V. Sergienko, "Theory of two-photon entanglement in type-II optical parametric down-conversion," Phys. Rev. A **50**, 5122–5133 (1994).
10. C. K. Hong and L. Mandel, "Theory of parametric frequency down conversion of light," Phys. Rev. A **31**, 2409–2418 (1985).

11. G. Brida, M. Chekhova, M. Genovese, and L. Krivitsky, "Generation of different bell state within spontaneous parametric down-conversion phase-matching bandwidth," Phys. Rev. A **76**, 053807 (2007)
12. G. Brida, M. V. Chekhova, M. Genovese, and L. A. Krivitsky, "Two-photon entanglement generation: different Bell states within the linewidth of phase-matching," Opt. Express **15**, 10182–10188 (2007)
13. A. V. Smith, SNLO nonlinear optics software, Sandia National Laboratories, http://www.sandia.gov/imrl/X1118/xxtal.htm.
14. A. Yariv and P. Yeh, *Optical Waves in Crystals* (Wiley, 2003), pp. 69–120.
15. A. Joobeur, B. E. A. Saleh, T. S. Larchuk, and M. C. Teich, "Coherence properties of entangled light beams generated by parametric down-conversion: theory and experiment," Phys. Rev. A **53**, 4360–4371 (1996)
16. K. Blushs and M. Auzinsh, "Validity of rate equations for Zeeman coherences for analysis of nonlinear interaction of atoms with broadband laser radiation," Phys. Rev. A **69**, 063806 (2004).